Observation of the Doubly Charmed Baryon Ξ_{cc}^+ with the LHCb Run 3 Detector

R. Aaij *et al.*[*]
(LHCb Collaboration)

(Received 31 March 2026; revised 7 May 2026; accepted 9 June 2026; published 8 July 2026)

The first observation of the doubly charmed baryon Ξ_{cc}^+ is reported through its decay to the $\Lambda_c^+ K^- \pi^+$ final state, with a statistical significance exceeding seven standard deviations. The observation is made using proton-proton collision data collected in 2024 with the LHCb Run 3 detector at a center-of-mass energy of 13.6 TeV, corresponding to a total integrated luminosity of 6.9 fb^{-1}. The Ξ_{cc}^+ mass is measured to be $3619.97 \pm 0.83 \pm 0.26^{+1.90}_{-1.30}$ MeV$/c^2$, where the first uncertainty is statistical, the second is systematic, and the third is due to the unknown Ξ_{cc}^+ lifetime, which is assumed to lie in the range 15–160 fs with a baseline value of 45 fs. The difference between the masses of the Ξ_{cc}^+ and Ξ_{cc}^{++} baryons is determined to be $-1.77 \pm 0.84 \pm 0.15^{+1.90}_{-1.30}$ MeV$/c^2$. This is the first observation of a new particle made with the LHCb Run 3 detector.

DOI: 10.1103/dmv6-7gdv

In the constituent quark model [1,2], the Ξ_{cc}^+ baryon is the isospin partner to the Ξ_{cc}^{++} baryon (with quark content $\Xi_{cc}^+ = ccd$ and $\Xi_{cc}^{++} = ccu$), just like the neutron (udd) to the proton (uud), and therefore, has approximately the same production cross section as the well-established Ξ_{cc}^{++} baryon [3–12]. Unlike the neutron, which is more massive than the proton by about 1.3 MeV$/c^2$ [13], the Ξ_{cc}^+ baryon is expected to have a smaller mass than the Ξ_{cc}^{++} baryon by a few MeV$/c^2$, due to the competition between electromagnetic and isospin-breaking effects [14–18]. The masses of both Ξ_{cc}^+ and Ξ_{cc}^{++} baryons have been predicted by various theoretical models [4,14–47], and the Ξ_{cc}^{++} mass has been measured to be 3621.55 ± 0.38 MeV$/c^2$ [48]. The Ξ_{cc}^+ lifetime is predicted to be three to six times shorter than the Ξ_{cc}^{++} lifetime, due to the W-exchange contribution in the Ξ_{cc}^+ decay and the constructive (destructive) Pauli interference of the $\Xi_{cc}^+(\Xi_{cc}^{++})$ decay amplitudes [4,20,26,36,49–56]. After considering the measured Ξ_{cc}^{++} lifetime to be 256 ± 27 fs [57], the Ξ_{cc}^+ lifetime is assumed to lie in the range 36–138 fs. The first theoretical prediction accounting for higher-order contributions gives a Ξ_{cc}^+ lifetime of 45 fs [55], and this value is used as the baseline for the simulation in this analysis.

The Ξ_{cc}^+ baryon has been searched for by several experiments in the past decades. The SELEX Collaboration claimed an observation of the Ξ_{cc}^+ baryon decaying into the $\Lambda_c^+ K^- \pi^+$ and $D^+ p K^-$ final states [58,59], using a 600 GeV$/c$ charged hyperon beam impinging on a fixed target. The mass of the Ξ_{cc}^+ baryon, averaged over the two decay modes, was found to be 3518.7 ± 1.7 MeV$/c^2$, and the lifetime was measured to be less than 33 fs at the 90% confidence level. It was estimated that about 20% of Λ_c^+ baryons in the SELEX experiment were produced from Ξ_{cc}^+ decays [58]. Searches in different production environments by the FOCUS [60], *BABAR* [61], LHCb [62–64], and Belle [65] Collaborations did not confirm the SELEX results. Meanwhile, the Ξ_{cc}^{++} baryon was observed by the LHCb experiment in the $\Lambda_c^+ K^- \pi^+ \pi^+$ final state [66] and confirmed in the $\Xi_c^+ \pi^+$ final state [67]. The Ξ_{cc}^{++} mass was measured in these decay modes to be about 100 MeV$/c^2$ higher than the mass of the Ξ_{cc}^+ baryon claimed by SELEX, in contradiction to the theoretical expectation noted above. Recently, the LHCb collaboration has observed two additional decay modes of the Ξ_{cc}^{++} baryon, namely, $\Xi_{cc}^{++} \to \Xi_c'^+ \pi^+$ [68] and $\Xi_{cc}^{++} \to \Xi_c^0 \pi^+ \pi^+$ [69].

This Letter presents a search for the Ξ_{cc}^+ baryon via the decay mode $\Xi_{cc}^+ \to \Lambda_c^+ K^- \pi^+$, where the Λ_c^+ baryon is reconstructed in the final state $pK^-\pi^+$. An example Feynman diagram of the decay is shown in Fig. 1. The inclusion of charge-conjugate decay processes is implied throughout this Letter. The dataset comprises proton-proton (pp) collision data recorded with the LHCb Run 3 detector in 2024 at a center-of-mass energy $\sqrt{s} = 13.6$ TeV, corresponding to an integrated luminosity of 6.9 fb^{-1}. To avoid experimenter bias, the results of the analysis were not examined until the full procedure had been finalized. The $\Xi_{cc}^{++} \to \Lambda_c^+ K^- \pi^+ \pi^+$ decay is used as a control mode to develop the event-selection strategy and to help calibrate a precision mass measurement.

The LHCb Run 3 detector [70] is a single-arm forward spectrometer covering the pseudorapidity range $2 < \eta < 5$,

[*]Full author list given at the end of the Letter.

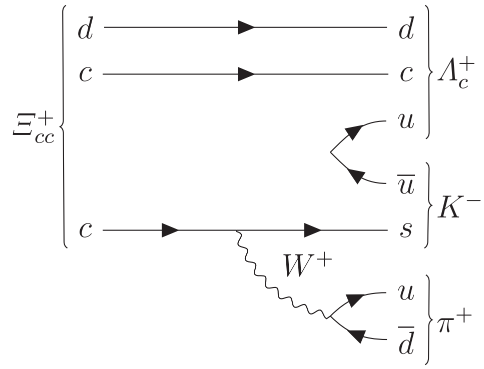

FIG. 1. Example Feynman diagram contributing to the decay $\Xi_{cc}^+ \to \Lambda_c^+ K^- \pi^+$.

designed for the study of particles containing b or c quarks. Installed prior to the start of Run 3 data taking in 2022, it represents a major upgrade of the detector. The new configuration has been designed to match the performance of the Run 1–2 detector [70,71], while allowing it to operate at approximately five times the instantaneous luminosity. The detector elements that are particularly relevant to this analysis include a silicon-pixel vertex detector surrounding the pp interaction region [72] that allows hadrons containing beauty or charm quarks to be identified from their characteristically long flight distances; a tracking system [73] that provides a measurement of the momentum, p, of charged particles; and two ring-imaging Cherenkov (RICH) detectors [74] that are able to discriminate between different species of charged hadrons. The readout of all detectors at the LHC collision frequency and the subsequent processing of the data in a full-software trigger [75–78] is a central feature of the upgraded detector, enabling the reconstruction and selection of events in real time. Compared with Run 2, the trigger efficiency of hadronic decay modes in the 2024 data taking has been improved by a factor of 2 to 4, depending on the number of final-state particles, thanks to the removal of the hardware trigger. The online reconstruction incorporates near-real-time alignment and calibration of the detector [79], which in turn allows the reconstruction of the $\Xi_{cc}^{+(+)}$ decays to be performed entirely by the trigger software. The momentum scale is calibrated using samples of $J/\psi \to \mu^+\mu^-$ and $B^+ \to J/\psi K^+$ decays collected concurrently with the data sample used for this analysis [80–82], and the calibration is applied offline along with the latest detector alignments. The relative accuracy of this procedure is estimated to be 2×10^{-4} using samples of other fully reconstructed heavy-flavor hadrons, including Υ and $\psi(2S)$ mesons.

Simulated samples of signal and control modes are required to model the effects of the detector acceptance and the imposed selection requirements. In the simulation, pp collisions are generated using PYTHIA 8 [83] with a specific LHCb configuration [84]. A dedicated generator, GENXICC2.0 [85], is used to simulate the doubly charmed baryon production and is interfaced to PYTHIA 8 to provide the underlying event, parton shower, and hadronization generation. Decays of unstable particles are described by EvtGen [86], in which final-state radiation is generated using PHOTOS [87]. The interaction of the generated particles with the detector and its response are simulated using the Geant4 toolkit [88] as described in Ref. [89]. Simulated $\Xi_{cc}^+ \to \Lambda_c^+ K^- \pi^+$ ($\Xi_{cc}^{++} \to \Lambda_c^+ K^- \pi^+ \pi^+$) samples are generated with a mass of 3621.4 MeV$/c^2$ and a lifetime of 45 fs [55,56] (256 fs [57]), and samples with different lifetime hypotheses are obtained using a weighting technique. Both Ξ_{cc}^+ and Ξ_{cc}^{++} baryon decays are generated uniformly within the allowed phase space.

Candidate $\Lambda_c^+ \to p K^- \pi^+$ decays are reconstructed from three charged particles identified as a proton, kaon, and pion using information from the RICH detectors. The particles are required to form a good-quality vertex and be inconsistent with originating from any primary pp collision vertex (PV). The Λ_c^+ candidate is required to have a mass in the range from 2270 to 2306 MeV$/c^2$, which corresponds to three times the mass resolution around its known mass. The Λ_c^+ candidate is then combined with two (three) additional charged particles to form a $\Xi_{cc}^+(\Xi_{cc}^{++})$ candidate. These additional particles must form a good-quality vertex with the Λ_c^+ candidate, and this vertex is required to be upstream of the Λ_c^+ decay vertex. Each $\Xi_{cc}^{+(+)}$ candidate is required to have a transverse momentum $p_T > 3$ GeV$/c$ and to be consistent with originating from its associated PV, defined as the PV with respect to which it has the smallest impact parameter (IP). To avoid candidates including duplicated segments of tracks, all track pairs are required to have an opening angle larger than 0.7 mrad.

In order to improve the signal purity, multivariate classifiers are trained to separate signal from background. First, a classifier based on a boosted decision tree (BDT) algorithm [90,91] implemented in the TMVA toolkit [92] is developed to select Λ_c^+ candidates. To mitigate the effects of the slightly different distributions of particle-identification variables in data and simulation, the classifier is trained directly on data. The signal proxy consists of Λ_c^+ candidates from a subset of data, with the background statistically subtracted using the *sPlot* technique [93], while candidates from the Λ_c^+ mass sidebands are used as a background proxy. The Λ_c^+ BDT response is then included in the training of a second BDT classifier used for the $\Xi_{cc}^{+(+)}$ decay selection. It uses simulated signal events as a signal proxy and wrong-sign (WS) $\Lambda_c^+ K^- \pi^-$ combinations in the mass range 3600–3640 MeV$/c^2$ in data as a background proxy. Both the signal and background proxies are required to satisfy all previous selection requirements. Variables used in the BDT training include the Ξ_{cc}^+ decay-vertex fit quality, the Ξ_{cc}^+ IP significance, the angle between the Ξ_{cc}^+ momentum and displacement vector from the associated PV, and the flight-distance χ^2 between the PV and the decay vertex of the Ξ_{cc}^{+} candidate. The flight-distance χ^2 is defined as the χ^2 of the hypothesis that the decay vertex of the candidate coincides with its associated PV. Variables associated with the decay products of the Ξ_{cc}^{+} candidates used in the BDT training include their p_{T} and IP significance, the vertex-fit quality of the Λ_c^{+} candidates, and the p_{T} and IP significance of the Λ_c^{+} decay products. Particle-identification information of the final-state particles from the Ξ_{cc}^{+} decay is also used.

The requirement applied to the classifier response is determined by maximizing the expected value of the figure of merit $\varepsilon/(\frac{5}{2}+\sqrt{B})$ [94], where ε is the estimated signal efficiency from simulation and B is the number of WS background candidates within $\pm 2\sigma_m$ from the expected signal mass. Here, $\sigma_m = 5.36\ \mathrm{MeV}/c^2$ is the mass resolution obtained from simulation and corrected for a 3% data-simulation difference measured with the Ξ_{cc}^{++} control sample. The performance of the multivariate selection is also tested on simulated signal candidates under other lifetime hypotheses and is found to have no strong dependence on this input.

The multivariate classifier for the $\Xi_{cc}^{++} \to \Lambda_c^+ K^- \pi^+ \pi^+$ decay is developed following the same strategy as that for the $\Xi_{cc}^{+} \to \Lambda_c^+ K^- \pi^+$ decay, except that the threshold of the classifier response is determined by maximizing the signal significance $S/\sqrt{S+B}$, where S is the expected signal yield, and B is the expected number of background candidates under the signal peak.

After the selection, an event may contain more than one $\Xi_{cc}^{+(+)}$ candidate. According to studies on simulated decays and the WS control sample, multiple candidates in the same event have very similar $\Xi_{cc}^{+(+)}$ mass if they are obtained from the same final-state tracks, but with two such tracks exchanged (e.g., the K^- from the Λ_c^+ decay and the K^- from the $\Xi_{cc}^{+(+)}$ decay). In this case, one candidate is chosen arbitrarily. Other kinds of multiple candidates, which account for 2% (7%) of the selected $\Xi_{cc}^{+}(\Xi_{cc}^{++})$ candidates in the mass fit window, are not removed [95], since they do not form a peaking background.

To improve the mass resolution, the invariant mass of $\Xi_{cc}^{+(+)}$ candidates is computed as

$$m_{\mathrm{cand}}(\Xi_{cc}^{+(+)}) = m[\Lambda_c^+ K^- \pi^+ (\pi^+)] - m([pK^-\pi^+]_{\Lambda_c^+}) + M_{\mathrm{PDG}}(\Lambda_c^+), \tag{1}$$

where $m[\Lambda_c^+ K^- \pi^+ (\pi^+)]$ is the reconstructed $\Xi_{cc}^{+(+)}$ mass; $m([pK^-\pi^+]_{\Lambda_c^+})$ is the reconstructed Λ_c^+ mass; and $M_{\mathrm{PDG}}(\Lambda_c^+)$ is the known Λ_c^+ mass, $2286.46 \pm 0.14\ \mathrm{MeV}/c^2$ [96].

The $m_{\mathrm{cand}}(\Xi_{cc}^{++})$ distribution of the selected Ξ_{cc}^{++} candidates in data is shown in Fig. 2. An unbinned extended maximum-likelihood fit to the distribution is performed as in Ref. [48], with the signal described by a crystal ball function [97] and the background parametrized by an exponential function. The fitted signal yield is 8712 ± 160, while the fitted mass is $3621.93 \pm 0.10\ \mathrm{MeV}/c^2$, where the uncertainties are statistical only. The Ξ_{cc}^{++} signal yield per fb^{-1} of data was 1262 in 2024, compared with 285 in the Run 2 data [48], which means that the efficiency in 2024 had increased by a factor of about 4 compared with Run 2.

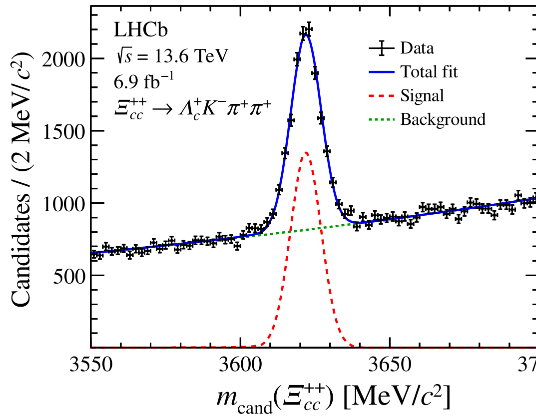

FIG. 2. Mass distribution of the selected Ξ_{cc}^{++} candidates in data, with fit results shown.

Multiple scattering can alter the values of the reconstructed mass and flight distance of the $\Xi_{cc}^{+(+)}$ candidates. Since the selection is more efficient for candidates with larger reconstructed flight distances, and the flight distance is correlated with the mass by the effect of multiple scattering, this can bias the $\Xi_{cc}^{+(+)}$ mass measurement. This effect is studied with charmed hadrons and is found to be well reproduced by simulation [48,66]. The corresponding corrections of $-0.26 \pm 0.03\ \mathrm{MeV}/c^2$ for the Ξ_{cc}^{++} mass and $-2.0 \pm 0.1\ \mathrm{MeV}/c^2$ for the Ξ_{cc}^{+} mass (assuming a lifetime of 45 fs) are determined using simulated samples by comparing the fitted mass of signal candidates before and after applying the selection. Final-state photon radiation also causes a bias in the measured mass. It is determined with the simulation [87] to be $-0.07 \pm 0.10\ \mathrm{MeV}/c^2$ and $-0.14 \pm 0.10\ \mathrm{MeV}/c^2$ for the Ξ_{cc}^{++} [48] and Ξ_{cc}^{+} baryons, respectively. These corrections are applied to the fitted mass values. The uncertainties are due to the limited size of simulated samples and are taken as systematic uncertainties on the $\Xi_{cc}^{+(+)}$ mass. After correcting for the bias due to the event selection and final-state radiation, the Ξ_{cc}^{++} mass is determined to be $3621.74 \pm 0.10\ \mathrm{MeV}/c^2$, where the uncertainty is statistical only. This is consistent with the Ξ_{cc}^{++} mass obtained from LHCb Run 1–2 data, $3621.6 \pm 0.4\ \mathrm{MeV}/c^2$ [48].

The $m_{\mathrm{cand}}(\Xi_{cc}^{+})$ distributions of the selected Ξ_{cc}^{+} candidates for the right-sign (RS) and WS data samples are shown in Fig. 3. A structure is visible in the signal mode at a mass of approximately $3620\ \mathrm{MeV}/c^2$. No significant structure is visible in the WS control sample. To measure the properties of the structure, an unbinned extended

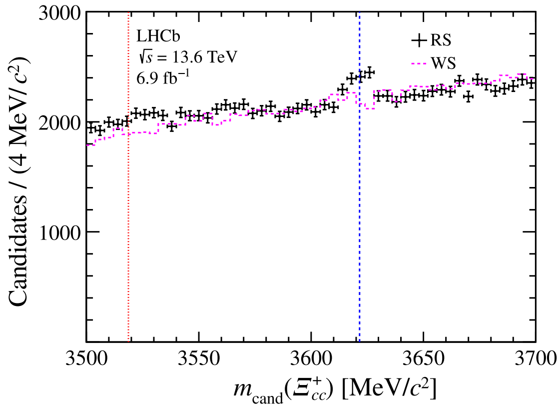

FIG. 3. Mass distributions of the selected Ξ_{cc}^+ candidates. The RS $m(\Lambda_c^+ K^- \pi^+)$ distribution is shown along with the WS $m(\Lambda_c^+ K^- \pi^-)$ distribution. The dotted red line at 3518.7 MeV$/c^2$ indicates the mass of the Ξ_{cc}^+ baryon claimed by SELEX [58,59], and the dashed blue line at 3621.6 MeV$/c^2$ indicates the mass of the isospin partner, the Ξ_{cc}^{++} baryon [48].

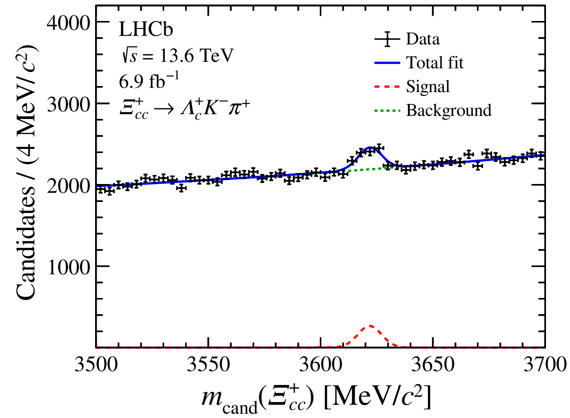

FIG. 4. Mass distribution of the selected Ξ_{cc}^+ candidates in data with fit results shown.

maximum-likelihood fit is performed to the mass distribution in the $\Lambda_c^+ K^- \pi^+$ mass window of 3500–3700 MeV$/c^2$ (Fig. 4). This choice excludes the partially reconstructed background, e.g., from $\Xi_{cc}^{++} \to \Lambda_c^+ K^- \pi^+ \pi^+$ decays with one of the pions from the Ξ_{cc}^{++} decay missing. The peaking structure is described by a crystal ball function with all parameters fixed from simulation with the exception of the peak position and the yield. The mass resolution is fixed to 5.36 MeV$/c^2$, as obtained from simulation, and corrected for a 3% data-simulation difference measured with the Ξ_{cc}^{++} control sample. The background is described by a second-order polynomial function with parameters free to vary in the fit. The signal yield is measured to be 915 ± 120, corresponding to a local statistical significance in excess of seven standard deviations (σ) when evaluated with a likelihood-ratio test for rejection of the background-only hypothesis [98,99].

The same structure is also seen in a pp data sample collected by LHCb at $\sqrt{s} = 13$ TeV in 2016–2018 data (part of Run 2), as shown in the End Matter. The signal yield in that sample is measured to be 304 ± 80, corresponding to a statistical significance of 4σ, and the mass value is consistent with that obtained in the data sample used for this analysis. Compared with Run 2, the signal yield of the $\Xi_{cc}^+ \to \Lambda_c^+ K^- \pi^+$ decay normalized by the integrated luminosity in 2024 is larger by only a factor of about 2.5, instead of 4 for the Ξ_{cc}^{++} baryon. This is mainly due to the smaller lifetime of the Ξ_{cc}^+ baryon; therefore, the event selection relies more on the momenta instead of the lifetime-related variables and is less affected by the momentum thresholds in the hardware trigger of Run 2.

Additional cross-checks are performed to test the robustness of the signal. These include changing the background line shape to an exponential function, letting the mass resolution float freely, and using an alternative multivariate classifier for Ξ_{cc}^+ without including particle-identification information in the training. In each of the tests, the significance of the structure in the $\Lambda_c^+ K^- \pi^+$ final state remains above 6σ.

The sources of systematic uncertainty affecting the measurement of the Ξ_{cc}^+ mass, $M(\Xi_{cc}^+)$, and the mass difference between the Ξ_{cc}^+ and Ξ_{cc}^{++} baryons, $\Delta M \equiv M(\Xi_{cc}^+) - M(\Xi_{cc}^{++})$, include the effects of the momentum-scale calibration, the energy loss [100], the selection, the invariant-mass fit model, the uncertainty on the Λ_c^+ mass, and the unknown Ξ_{cc}^+ lifetime. They are summarized in Table I. After the momentum-scale calibration, an uncertainty of $\pm 0.02\%$ is assigned, which is estimated by using samples of Υ and $\psi(2S)$ decays. The energy loss is evaluated following Ref. [100] by studying the fitted mass of $\psi(2S) \to J/\psi \pi^+ \pi^-$ decays as a function of the momentum of the pair of pions to determine the bias. The bias on the Ξ_{cc}^+ mass due to the selection is estimated using simulation and has uncertainty due to the limited size of the simulation sample. Such bias depends on the unknown Ξ_{cc}^+ lifetime, which introduces a further source of uncertainty on the correction. This uncertainty is estimated by repeating the analysis for other Ξ_{cc}^+ lifetime hypotheses between 15 and 160 fs (adding approximately

TABLE I. Systematic uncertainties on $M(\Xi_{cc}^+)$ and the mass difference $\Delta M \equiv M(\Xi_{cc}^+) - M(\Xi_{cc}^{++})$.

Source	$M(\Xi_{cc}^+)$ [MeV$/c^2$]	ΔM [MeV$/c^2$]
Momentum-scale calibration	0.14	0.03
Energy loss	0.10	0.05
Selection bias correction	0.10	0.10
Mass fit model	0.10	0.10
Λ_c^+ mass uncertainty	0.14	...
Sum in quadrature	0.26	0.15
Ξ_{cc}^+ lifetime	${}^{+1.90}_{-1.30}$	${}^{+1.90}_{-1.30}$

20 fs on both sides of the predicted range, 36–138 fs). The bias is estimated to be $+3.3 \pm 0.2$ MeV/c^2 for 15 fs and $+0.1 \pm 0.1$ MeV/c^2 for 160 fs, respectively. These correspond to an additional correction of -1.3 MeV/c^2 for 15 fs and $+1.9$ MeV/c^2 for 160 fs and are listed separately. The dependence of the measurement on the mass fit model is estimated by varying the shape parameters that are fixed according to simulation, by using alternative signal and background models (a double crystal ball function as signal or an exponential function as background), and by repeating the fits in different mass ranges. The largest deviation in the results is assigned as a systematic uncertainty. Finally, since the Ξ_{cc}^{+} mass is measured relative to the Λ_c^+ mass, the uncertainty of 0.14 MeV/c^2 on the world-average value [96] of the latter is included. The total systematic uncertainty is obtained as the sum in quadrature of these uncertainties.

In summary, a significant structure that is consistent with the Ξ_{cc}^{+} baryon is observed in the final state $\Lambda_c^+ K^- \pi^+$ in a pp data sample collected with the LHCb Run 3 detector during 2024 at a center-of-mass energy of 13.6 TeV, with a signal yield of 915 ± 120. The mass of the structure is measured to be

$$M(\Xi_{cc}^{+}) = 3619.97 \pm 0.83 \pm 0.26^{+1.90}_{-1.30}\ \mathrm{MeV}/c^2,$$

where the first uncertainty is statistical, the second is systematic, and the third is due to the unknown Ξ_{cc}^{+} lifetime, which is assumed to lie in the range 15–160 fs with a baseline value of 45 fs. A measurement of the Ξ_{cc}^{+} lifetime would significantly reduce the latter uncertainty. The mass difference between the Ξ_{cc}^{+} and Ξ_{cc}^{++} states is determined to be

$$\Delta M = -1.77 \pm 0.84 \pm 0.15^{+1.90}_{-1.30}\ \mathrm{MeV}/c^2,$$

which is consistent with theoretical predictions [14–18] that include partial cancellation of QCD and QED effects. The mass of the observed Ξ_{cc}^{+} state is greater than that of the Ξ_{cc}^{+} state claimed by the SELEX Collaboration [58,59] by 101 ± 2 MeV/c^2 and consistent with the value corresponding to the local excess found in previous LHCb searches based on the Run 1 and Run 2 samples [63,64]. Consequently, the interpretation of the SELEX state as the Ξ_{cc}^{+} baryon is not supported.

This observation was made possible thanks to a significant increase in the selection efficiency for this channel in the 2024 data sample compared with Run 2, stemming from the enhanced capabilities of the upgraded LHCb detector and its trigger system.

Acknowledgments—We express our gratitude to our colleagues in the CERN accelerator departments for the excellent performance of the LHC. We thank the technical and administrative staff at the LHCb institutes. We acknowledge support from CERN and from the national agencies: ARC (Australia); CAPES, CNPq, FAPERJ, and FINEP (Brazil); MOST and NSFC (China); CNRS/IN2P3 and CEA (France); BMFTR, DFG, and MPG (Germany); INFN (Italy); NWO (Netherlands); MNiSW and NCN (Poland); MEC/IFA (Romania); MICIU and AEI (Spain); SNSF and SER (Switzerland); NASU (Ukraine); STFC (United Kingdom); DOE NP and NSF (USA). We acknowledge the computing resources that are provided by ARDC (Australia), CBPF (Brazil), CERN, IHEP, and LZU (China), IN2P3 (France), KIT and DESY (Germany), INFN (Italy), SURF (Netherlands), Polish WLCG (Poland), IFIN-HH (Romania), PIC (Spain), CSCS (Switzerland), GridPP (United Kingdom), and NSF (USA). We are indebted to the communities behind the multiple open-source software packages on which we depend. Individual groups or members have received support from RTP (Australia); Key Research Program of Frontier Sciences of CAS, CAS PIFI, CAS CCEPP (China); Minciencias (Colombia); EPLANET, Marie Skłodowska-Curie Actions, ERC, and NextGenerationEU (European Union); A*MIDEX, ANR, IPhU, Labex P2IO, and Région Auvergne-Rhône-Alpes (France); Alexander-von-Humboldt Foundation (Germany); ICSC (Italy); Severo Ochoa and María de Maeztu Units of Excellence, GVA, XuntaGal, GENCAT, InTalent-Inditex and Prog. Atracción Talento CM (Spain); the Leverhulme Trust, the Royal Society, and UKRI (United Kingdom).

Data availability—The data that support the findings of this article are openly available [101].

[1] M. Gell-Mann, A schematic model of baryons and mesons, Phys. Lett. **8**, 214 (1964).

[2] G. Zweig, An SU_3 model for strong interaction symmetry and its breaking; Version 1, Report No. CERN-TH-401, CERN, Geneva, 1964; An SU_3 model for strong interaction symmetry and its breaking; Version 2, Report No. CERN-TH-412, CERN, Geneva, 1964.

[3] A. V. Berezhnoy, V. V. Kiselev, A. K. Likhoded, and A. I. Onishchenko, Doubly charmed baryon production in hadronic experiments, Phys. Rev. D **57**, 4385 (1998).

[4] V. V. Kiselev and A. K. Likhoded, Baryons with two heavy quarks, Phys. Usp. **45**, 455 (2002).

[5] J. P. Ma and Z. G. Si, Factorization approach for inclusive production of doubly heavy baryon, Phys. Lett. B **568**, 135 (2003).

[6] C.-H. Chang, J.-P. Ma, C.-F. Qiao, and X.-G. Wu, Hadronic production of the doubly charmed baryon Ξ_{cc} with intrinsic charm, J. Phys. G **34**, 845 (2007).

[7] C.-H. Chang, C.-F. Qiao, J.-X. Wang, and X.-G. Wu, Estimate of the hadronic production of the doubly charmed baryon Ξ_{cc} in the general-mass variable-flavor-number scheme, Phys. Rev. D **73**, 094022 (2006).

[8] J.-W. Zhang, X. G. Wu, T. Zhong, Y. Yu, and Z. Y. Fang, Hadronic production of the doubly heavy baryon Ξ_{bc} at LHC, Phys. Rev. D **83**, 034026 (2011).

[9] C.-H. Chang, C.-F. Qiao, J.-X. Wang, and X.-G. Wu, The color-octet contributions to P-wave B_c meson hadroproduction, Phys. Rev. D **71**, 074012 (2005).

[10] Z. Sun and X.-G. Wu, The production of the doubly charmed baryon in deeply inelastic ep scattering at the Large Hadron Electron Collider, J. High Energy Phys. 07 (2020) 034.

[11] H. Yang, J. Jiang, and B. Long, Doubly heavy hadron production in ultraperipheral collision, Phys. Rev. D **109**, 114034 (2024).

[12] X.-Y. Zhao, L. Guo, X.-C. Zheng, H.-Y. Bi, X.-G. Wu, and Q.-W. Ke, Production of doubly heavy baryon at the muon-ion collider, Chin. Phys. C **49**, 053103 (2025).

[13] E. Tiesinga, P. J. Mohr, D. B. Newell, and B. N. Taylor, CODATA recommended values of the fundamental physical constants: 2018*, Rev. Mod. Phys. **93**, 025010 (2021).

[14] C.-W. Hwang and C.-H. Chung, Isospin mass splittings of heavy baryons in heavy quark symmetry, Phys. Rev. D **78**, 073013 (2008).

[15] S. J. Brodsky, F.-K. Guo, C. Hanhart, and U.-G. Meißner, Isospin splittings of doubly heavy baryons, Phys. Lett. B **698**, 251 (2011).

[16] S. Borsanyi *et al.* (BMW Collaboration), *Ab initio* calculation of the neutron-proton mass difference, Science **347** (2015) 1452.

[17] K.-W. Wei, B. Chen, and X.-H. Guo, Masses of doubly and triply charmed baryons, Phys. Rev. D **92**, 076008 (2015).

[18] M. Karliner and J. L. Rosner, Isospin splittings in baryons with two heavy quarks, Phys. Rev. D **96**, 033004 (2017).

[19] B. O. Kerbikov, M. I. Polikarpov, and L. V. Shevchenko, Multiquark masses and wave functions through a modified green function Monte Carlo method, Nucl. Phys. **B331**, 19 (1990).

[20] S. Fleck and J.-M. Richard, Baryons with double charm, Prog. Theor. Phys. **82**, 760 (1989).

[21] J. G. Körner, M. Krämer, and D. Pirjol, Heavy baryons, Prog. Part. Nucl. Phys. **33**, 787 (1994).

[22] S. Chernyshev, M. A. Nowak, and I. Zahed, Heavy hadrons and QCD instantons, Phys. Rev. D **53**, 5176 (1996).

[23] D. Ebert, R. N. Faustov, V. O. Galkin, A. P. Martynenko, and V. A. Saleev, Heavy baryons in the relativistic quark model, Z. Phys. C **76**, 111 (1997).

[24] S. S. Gershtein, V. V. Kiselev, A. K. Likhoded, and A. I. Onishchenko, Spectroscopy of doubly charmed baryons: Ξ_{cc}^{+} and Ξ_{cc}^{++}, Mod. Phys. Lett. A **14**, 135 (1999); S. S. Gershtein, V. V. Kiselev, A. K. Likhoded, and A. I. Onishchenko, Spectroscopy of doubly heavy baryons, Phys. At. Nucl. **63**, 274 (2000); Yad. Fiz. **63**, 334 (2000); Phys. Rev. D **62**, 054021 (2000).

[25] C. Itoh, T. Minamikawa, K. Miura, and T. Watanabe, Doubly charmed baryon masses and quark wave functions in baryons, Phys. Rev. D **61**, 057502 (2000).

[26] K. Anikeev *et al.*, B physics at the Tevatron: Run II and beyond, in *Workshop on B physics at the Tevatron: Run II and beyond, Batavia, Illinois* (1999).

[27] D. Ebert, R. N. Faustov, V. O. Galkin, and A. P. Martynenko, Mass spectra of doubly heavy baryons in the relativistic quark model, Phys. Rev. D **66**, 014008 (2002).

[28] N. Mathur, R. Lewis, and R. M. Woloshyn, Charmed and bottom baryons from lattice nonrelativistic QCD, Phys. Rev. D **66**, 014502 (2002).

[29] D.-H. He, K. Qian, Y. B. Ding, X. Q. Li, and P. N. Shen, Evaluation of the spectra of baryons containing two heavy quarks in a bag model, Phys. Rev. D **70**, 094004 (2004).

[30] W. Roberts and M. Pervin, Heavy baryons in a quark model, Int. J. Mod. Phys. A **23**, 2817 (2008).

[31] A. Valcarce, H. Garcilazo, and J. Vijande, Towards an understanding of heavy baryon spectroscopy, Eur. Phys. J. A **37**, 217 (2008).

[32] J.-R. Zhang and M.-Q. Huang, Doubly heavy baryons in QCD sum rules, Phys. Rev. D **78**, 094007 (2008).

[33] Z.-G. Wang, Analysis of the $\frac{1}{2}^{+}$ doubly heavy baryon states with QCD sum rules, Eur. Phys. J. A **45**, 267 (2010).

[34] T. M. Aliev, K. Azizi, and M. Savcı, Doubly heavy spin-$1/2$ baryon spectrum in QCD, Nucl. Phys. **A895**, 59 (2012).

[35] Y. Namekawa *et al.* (PACS-CS Collaboration), Charmed baryons at the physical point in $2+1$ flavor lattice QCD, Phys. Rev. D **87**, 094512 (2013).

[36] M. Karliner and J. L. Rosner, Baryons with two heavy quarks: Masses, production, decays, and detection, Phys. Rev. D **90**, 094007 (2014).

[37] Z. S. Brown, W. Detmold, S. Meinel, and K. Orginos, Charmed bottom baryon spectroscopy from lattice QCD, Phys. Rev. D **90**, 094507 (2014).

[38] Z.-F. Sun, Z.-W. Liu, X. Liu, and S.-L. Zhu, Masses and axial currents of the doubly charmed baryons, Phys. Rev. D **91**, 094030 (2015).

[39] M. Padmanath, R. G. Edwards, N. Mathur, and M. Peardon (Hadron Spectrum Collaboration), Spectroscopy of doubly charmed baryons from lattice QCD, Phys. Rev. D **91**, 094502 (2015).

[40] P. Pérez-Rubio, S. Collins, and G. S. Bali, Charmed baryon spectroscopy and light flavor symmetry from lattice QCD, Phys. Rev. D **92**, 034504 (2015).

[41] Z.-F. Sun and M. J. Vicente Vacas, Masses of doubly charmed baryons in the extended on-mass-shell renormalization scheme, Phys. Rev. D **93**, 094002 (2016).

[42] C. Alexandrou and C. Kallidonis, Low-lying baryon masses using $N_f = 2$ twisted mass clover-improved fermions directly at the physical pion mass, Phys. Rev. D **96**, 034511 (2017).

[43] Y. Liu and I. Zahed, Heavy baryons and their exotics from instantons in holographic QCD, Phys. Rev. D **95**, 116012 (2017); Heavy and strange holographic baryons, Phys. Rev. D **96**, 056027 (2017).

[44] Z. Ghalenovi, C.-P. Shen, and M. Moazzen Sorkhi, Mass spectra and semileptonic decays of doubly heavy Ξ and Ω baryons, Phys. Lett. B **834**, 137405 (2022).

[45] G.-L. Yu, Y. Meng, Z.-Y. Li, Z.-G. Wang, and L. Jie, Systematic analysis of doubly charmed baryons Ξ_{cc} and Ω_{cc}, Eur. Phys. J. A **59**, 126 (2023).

[46] J.-H. Pan and J.-S. Pan, Study of the mass spectra of doubly heavy $\Xi_{QQ'}$ and $\Omega_{QQ'}$ baryons, Eur. Phys. J. C **85**, 1009 (2025).

[47] P. Jakhad and A. K. Rai, Relativistic flux tube model predictions from charmed mesons to double-charmed baryons, Phys. Rev. D **113**, 054046 (2026).
[48] R. Aaij *et al.* (LHCb Collaboration), Precision measurement of the Ξ_{cc}^{++} mass, J. High Energy Phys. 02 (2020) 049.
[49] B. Guberina, B. Melić, and H. Štefančić, Inclusive decays and lifetimes of doubly charmed baryons, Eur. Phys. J. C **9**, 213 (1999); **13**, 551(E) (2000).
[50] V. V. Kiselev, A. K. Likhoded, and A. I. Onishchenko, Lifetimes of doubly charmed baryons: Ξ_{cc}^{+} and Ξ_{cc}^{++}, Phys. Rev. D **60**, 014007 (1999).
[51] A. K. Likhoded and A. I. Onishchenko, Lifetimes of doubly heavy baryons, arXiv:hep-ph/9912425.
[52] A. I. Onishchenko, Inclusive and exclusive decays of doubly heavy baryons, arXiv:hep-ph/0006295.
[53] C.-H. Chang, T. Li, X.-Q. Li, and Y.-M. Wang, Lifetime of doubly charmed baryons, Commun. Theor. Phys. **49**, 993 (2008).
[54] A. V. Berezhnoy and A. K. Likhoded, Doubly heavy baryons, Phys. At. Nucl. **79**, 260 (2016).
[55] H.-Y. Cheng and Y.-L. Shi, Lifetimes of doubly charmed baryons, Phys. Rev. D **98**, 113005 (2018).
[56] L. Dulibić, J. Gratrex, B. Melić, and I. Nišandžić, Revisiting lifetimes of doubly charmed baryons, J. High Energy Phys. 07 (2023) 061.
[57] R. Aaij *et al.* (LHCb Collaboration), Measurement of the lifetime of the doubly charmed baryon Ξ_{cc}^{++}, Phys. Rev. Lett. **121**, 052002 (2018).
[58] M. Mattson *et al.* (SELEX Collaboration), First observation of the doubly charmed baryon Ξ_{cc}^{+}, Phys. Rev. Lett. **89**, 112001 (2002).
[59] A. Ocherashvili *et al.* (SELEX Collaboration), Confirmation of the double charm baryon $\Xi_{cc}^{+}(3520)$ via its decay to $pD^{+}K^{-}$, Phys. Lett. B **628**, 18 (2005).
[60] S. P. Ratti, New results on c-baryons and a search for cc-baryons in FOCUS, Nucl. Phys. B, Proc. Suppl. **115**, 33 (2003).
[61] B. Aubert *et al.* (*BABAR* Collaboration), Search for doubly charmed baryons Ξ_{cc}^{+} and Ξ_{cc}^{++} in *BABAR*, Phys. Rev. D **74**, 011103 (2006).
[62] R. Aaij *et al.* (LHCb Collaboration), Search for the doubly charmed baryon Ξ_{cc}^{+}, J. High Energy Phys. 12 (2013) 090.
[63] R. Aaij *et al.* (LHCb Collaboration), Search for the doubly charmed baryon Ξ_{cc}^{+}, Sci. China Phys. Mech. Astron. **63**, 221062 (2020).
[64] R. Aaij *et al.* (LHCb Collaboration), Search for the doubly charmed baryon Ξ_{cc}^{+} in the $\Xi_{c}^{+}\pi^{-}\pi^{+}$ final state, J. High Energy Phys. 12 (2021) 107.
[65] Y. Kato *et al.* (Belle Collaboration), Search for doubly charmed baryons and study of charmed strange baryons at Belle, Phys. Rev. D **89**, 052003 (2014).
[66] R. Aaij *et al.* (LHCb Collaboration), Observation of the doubly charmed baryon Ξ_{cc}^{++}, Phys. Rev. Lett. **119**, 112001 (2017).
[67] R. Aaij *et al.* (LHCb Collaboration), First observation of the doubly charmed baryon decay $\Xi_{cc}^{++} \to \Xi_{c}^{+}\pi^{+}$, Phys. Rev. Lett. **121**, 162002 (2018).
[68] R. Aaij *et al.* (LHCb Collaboration), Observation of the doubly charmed baryon decay $\Xi_{cc}^{++} \to \Xi_{c}^{\prime +}\pi^{+}$, J. High Energy Phys. 05 (2022) 038.
[69] R. Aaij *et al.* (LHCb Collaboration), Observation of the doubly-charmed-baryon decay $\Xi_{cc}^{++} \to \Xi_{c}^{0}\pi^{+}\pi^{+}$, J. High Energy Phys. 10 (2025) 136.
[70] R. Aaij *et al.* (LHCb Collaboration), The LHCb upgrade I, J. Instrum. **19**, P05065 (2024).
[71] A. A. Alves Jr. *et al.* (LHCb Collaboration), The LHCb detector at the LHC, J. Instrum. **3** (2008) S08005.
[72] LHCb Collaboration, LHCb VELO upgrade technical design report, Report No. CERN-LHCC-2013-021, CERN, 2013.
[73] LHCb Collaboration, LHCb tracker upgrade technical design report, Report No. CERN-LHCC-2014-001, CERN, 2014.
[74] LHCb Collaboration, LHCb PID upgrade technical design report, Report No. CERN-LHCC-2013-022, CERN, 2013.
[75] LHCb Collaboration, LHCb trigger and online upgrade technical design report, Report No. CERN-LHCC-2014-016, CERN, 2014.
[76] LHCb Collaboration, LHCb upgrade software and computing, Report No. CERN-LHCC-2018-007, CERN, 2018.
[77] LHCb Collaboration, Computing model of the upgrade LHCb experiment, Report No. CERN-LHCC-2018-014, CERN, 2018.
[78] LHCb Collaboration, LHCb upgrade GPU high level trigger technical design report, Report No. CERN-LHCC-2020-006, CERN, 2020.
[79] G. Dujany and B. Storaci, Real-time alignment and calibration of the LHCb detector in Run II, J. Phys. Conf. Ser. **664**, 082010 (2015).
[80] R. Aaij *et al.* (LHCb Collaboration), Measurements of the Λ_{b}^{0}, Ξ_{b}^{-}, and Ω_{b}^{-} baryon masses, Phys. Rev. Lett. **110**, 182001 (2013).
[81] R. Aaij *et al.* (LHCb Collaboration), Precision measurement of D meson mass differences, J. High Energy Phys. 06 (2013) 065.
[82] R. Aaij *et al.* (LHCb Collaboration), Momentum scale calibration of the LHCb spectrometer, J. Instrum. **19**, P02008 (2024).
[83] T. Sjöstrand, S. Mrenna, and P. Skands, A brief introduction to PYTHIA 8.1, Comput. Phys. Commun. **178**, 852 (2008); T. Sjöstrand, S. Mrenna, and P. Skands, PYTHIA 6.4 physics and manual, J. High Energy Phys. 05 (2006) 026.
[84] I. Belyaev *et al.*, Handling of the generation of primary events in Gauss, the LHCb simulation framework, J. Phys. Conf. Ser. **331**, 032047 (2011).
[85] C.-H. Chang, J.-X. Wang, and X.-G. Wu, GENXICC2.0: An upgraded version of the generator for hadronic production of double heavy baryons Ξ_{cc}, Ξ_{bc} and Ξ_{bb}, Comput. Phys. Commun. **181**, 1144 (2010).
[86] D. J. Lange, The EvtGen particle decay simulation package, Nucl. Instrum. Methods Phys. Res., Sect. A **462**, 152 (2001).
[87] N. Davidson, T. Przedzinski, and Z. Was, PHOTOS interface in C++: Technical and physics documentation, Comput. Phys. Commun. **199**, 86 (2016).
[88] J. Allison *et al.* (Geant4 Collaboration), Geant4 developments and applications, IEEE Trans. Nucl. Sci. **53**, 270

(2006); S. Agostinelli *et al.* (Geant4 Collaboration), Geant4: A simulation toolkit, Nucl. Instrum. Methods Phys. Res., Sect. A **506**, 250 (2003).

[89] M. Clemencic, G. Corti, S. Easo, C. R. Jones, S. Miglioranzi, M. Pappagallo, and P. Robbe, The LHCb simulation application, Gauss: Design, evolution and experience, J. Phys. Conf. Ser. **331**, 032023 (2011).

[90] L. Breiman, J. H. Friedman, R. A. Olshen, and C. J. Stone, *Classification and regression trees* (Wadsworth International Group, Belmont, California, 1984).

[91] Y. Freund and R. E. Schapire, A decision-theoretic generalization of on-line learning and an application to boosting, J. Comput. Syst. Sci. **55**, 119 (1997).

[92] H. Voss, A. Hoecker, J. Stelzer, and F. Tegenfeldt, TMVA—Toolkit for multivariate data analysis with ROOT, Proc. Sci. ACAT2007 (**2007**) 040; A. Hoecker *et al.*, TMVA 4—Toolkit for multivariate data analysis with ROOT. Users guide, arXiv:physics/0703039.

[93] M. Pivk and F. R. Le Diberder, sPlot: A statistical tool to unfold data distributions, Nucl. Instrum. Methods Phys. Res., Sect. A **555**, 356 (2005).

[94] G. Punzi, Sensitivity of searches for new signals and its optimization, eConf **C030908**, MODT002 (2003).

[95] P. Koppenburg, Statistical biases in measurements with multiple candidates, arXiv:1703.01128.

[96] B. Aubert *et al.* (*BABAR* Collaboration), A precision measurement of the Λ_c^+ baryon mass, Phys. Rev. D **72**, 052006 (2005).

[97] T. Skwarnicki, A study of the radiative cascade transitions between the Upsilon-prime and Upsilon resonances, Ph.D. thesis, Institute of Nuclear Physics, Krakow, 1986, DESY-F31-86-02.

[98] S. S. Wilks, The large-sample distribution of the likelihood ratio for testing composite hypotheses, Ann. Math. Stat. **9**, 60 (1938).

[99] G. Cowan, K. Cranmer, E. Gross, and O. Vitells, Asymptotic formulae for likelihood-based tests of new physics, Eur. Phys. J. C **71**, 1554 (2011).

[100] A. Chu, Y. Liu, and M. Needham, Improving systematic uncertainties on precision two-body mass measurements, EPJ Tech. Instrum. **13**, 3 (2026).

[101] https://cds.cern.ch/record/2959557.

End Matter

The Letter describes the observation of a narrow structure in the $\Lambda_c^+ K^- \pi^+$ mass spectrum in a sample of proton-proton data collected by the LHCb Run 3 detector in 2024 at a center-of-mass energy of 13.6 TeV, corresponding to an integrated luminosity of 6.9 fb^{-1}. As an additional cross-check, the Run 2 (2016–2018) data sample recorded by the LHCb experiment at a center-of-mass energy of 13 TeV as used in the previous search [63] has been reanalyzed using a previously unexplored data stream that selects $\Lambda_c^+ \to pK^-\pi^+$ inclusively. With this data stream, the transverse momentum requirements on the kaon and pion from the Ξ_{cc}^+ decay can be relaxed from 500 MeV/c to 200 MeV/c. An improved selection has been developed by including the particle-identification information in the multivariate analysis and taking into account that the Ξ_{cc}^+ lifetime was recently estimated to be about 45 fs [55,56], which is shorter than the assumed 80 fs in Ref. [63].

Figure 5 shows the Ξ_{cc}^+ mass spectrum in the Run 2 sample after the final selection. The fit procedure described in the Letter is applied to the selected candidates, with the mass resolution fixed to 6.28 MeV/c^2 as determined from simulation after correcting a difference of 10% between simulation and data found for the Ξ_{cc}^{++} baryon. The signal yield is measured to be 304 ± 80 and corresponds to a statistical significance of 4σ. The Ξ_{cc}^+ mass is determined to be 3620.8 ± 2.2 MeV/c^2, where the uncertainty is statistical only. This is consistent with the Ξ_{cc}^+ mass determined using 2024 data, $3619.97 \pm 0.83 \pm 0.26^{+1.90}_{-1.30}$ MeV/c^2.

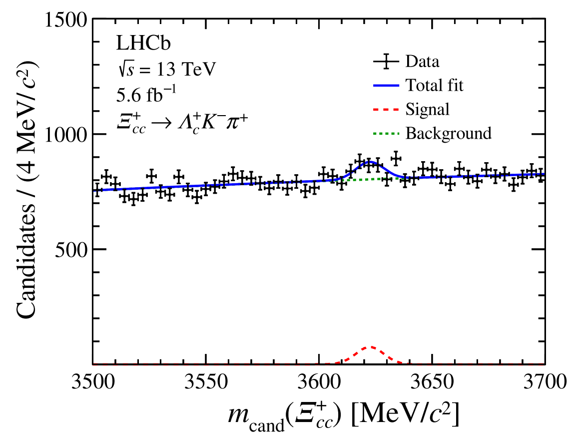

FIG. 5. Mass distribution of the selected Ξ_{cc}^+ candidates in Run 2 data, with the result of the fit also shown.

R. Aaij,[38] M. Abdelfatah,[69] A. S. W. Abdelmotteleb,[57] C. Abellan Beteta,[51] F. Abudinén,[59] T. Ackernley,[61] A. A. Adefisoye,[69] B. Adeva,[47] M. Adinolfi,[55] P. Adlarson,[87,42] C. Agapopoulou,[14] C. A. Aidala,[89] S. Akar,[11] K. Akiba,[38] P. Albicocco,[28] J. Albrecht,[19,b] R. Aleksiejunas,[81] F. Alessio,[49] P. Alvarez Cartelle,[47] S. Amato,[3] J. L. Amey,[55] Y. Amhis,[14] L. An,[6] L. Anderlini,[27] M. Andersson,[51] P. Andreola,[51] M. Andreotti,[26] S. Andres Estrada,[44] A. Anelli,[31,c] D. Ao,[7] C. Arata,[12] F. Archilli,[37] Z. Areg,[69] M. Argenton,[26] S. Arguedas Cuendis,[9,49] L. Arnone,[31,c] M. Artuso,[69] E. Aslanides,[13] R. Ataíde Da Silva,[50] M. Atzeni,[65] B. Audurier,[12] J. A. Authier,[15] D. Bacher,[64] I. Bachiller Perea,[50] S. Bachmann,[22] M. Bachmayer,[50] J. J. Back,[57] Z. B. Bai,[8] V. Balagura,[15] A. Balboni,[26] W. Baldini,[26] Z. Baldwin,[79] L. Balzani,[19] H. Bao,[7] J. Baptista de Souza Leite,[2] C. Barbero Pretel,[47,12] M. Barbetti,[27] I. R. Barbosa,[70] R. J. Barlow,[63,a] M. Barnyakov,[25] S. Baron,[49] S. Barsuk,[14] W. Barter,[59] J. Bartz,[69] S. Bashir,[40] B. Batsukh,[82] P. B. Battista,[14] A. Bavarchee,[80] A. Bay,[50] A. Beck,[65] M. Becker,[19] F. Bedeschi,[35] I. B. Bediaga,[2] N. A. Behling,[19] S. Belin,[47] A. Bellavista,[25] I. Belov,[29] I. Belyaev,[36] G. Bencivenni,[28] E. Ben-Haim,[16] J. L. M. Berkey,[68] R. Bernet,[51] A. Bertolin,[33] F. Betti,[59] J. Bex,[56] O. Bezshyyko,[88] S. Bhattacharya,[80] M. S. Bieker,[18] N. V. Biesuz,[26] A. Biolchini,[38] M. Birch,[62] F. C. R. Bishop,[10] A. Bitadze,[63] A. Bizzeti,[27,d] T. Blake,[57,e] F. Blanc,[50] J. E. Blank,[19] S. Blusk,[69] J. A. Boelhauve,[19] O. Boente Garcia,[49] T. Boettcher,[90] A. Bohare,[59] C. Bolognani,[19] R. Bolzonella,[26,f] R. B. Bonacci,[1] A. Bordelius,[49] F. Borgato,[33,49] S. Borghi,[63] M. Borsato,[31,c] J. T. Borsuk,[86] E. Bottalico,[61] S. A. Bouchiba,[50] M. Bovill,[64] T. J. V. Bowcock,[61] A. Boyer,[49] C. Bozzi,[26] J. D. Brandenburg,[91] A. Brea Rodriguez,[50] N. Breer,[19] C. Breitfeld,[19] J. Brodzicka,[41] J. Brown,[61] D. Brundu,[32] E. Buchanan,[59] M. Burgos Marcos,[84] C. Burr,[49] C. Buti,[27] J. S. Butter,[56] J. Buytaert,[49] W. Byczynski,[49] S. Cadeddu,[32] H. Cai,[75] Y. Cai,[5] A. Caillet,[16] R. Calabrese,[26,f] L. Calefice,[45] M. Calvi,[31,c] M. Calvo Gomez,[46] P. Camargo Magalhaes,[2,g] J. I. Cambon Bouzas,[47] P. Campana,[28] A. C. Campos,[3] A. F. Campoverde Quezada,[7] Y. Cao,[6] S. Capelli,[31,c] M. Caporale,[25] L. Capriotti,[33] R. Caravaca-Mora,[9] A. Carbone,[25,h] L. Carcedo Salgado,[47] R. Cardinale,[29,i] A. Cardini,[32] P. Carniti,[31] L. Carus,[22] A. Casais Vidal,[65] R. Caspary,[22] G. Casse,[61] M. Cattaneo,[49] G. Cavallero,[26] V. Cavallini,[26,f] S. Celani,[49] I. Celestino,[35,j] S. Cesare,[49,k] A. J. Chadwick,[61] I. Chahrour,[89] M. Charles,[16] Ph. Charpentier,[49] E. Chatzianagnostou,[38] R. Cheaib,[80] M. Chefdeville,[10] C. Chen,[57] J. Chen,[50] S. Chen,[5] Z. Chen,[7] A. Chen Hu,[62] M. Cherif,[12] S. Chernyshenko,[53] X. Chiotopoulos,[84] G. Chizhik,[1] V. Chobanova,[44] M. Chrzaszcz,[41] V. Chulikov,[28,36,49] P. Ciambrone,[28] X. Cid Vidal,[47] P. Cifra,[49] P. E. L. Clarke,[59] M. Clemencic,[49] H. V. Cliff,[56] J. Closier,[49] C. Cocha Toapaxi,[22] V. Coco,[49] J. Cogan,[13] E. Cogneras,[11] L. Cojocariu,[43] S. Collaviti,[50] P. Collins,[49] T. Colombo,[49] M. Colonna,[19] A. Comerma-Montells,[45] L. Congedo,[24] J. Connaughton,[57] A. Contu,[32] N. Cooke,[60] G. Cordova,[35,j] C. Coronel,[66] I. Corredoira,[12] A. Correia,[16] G. Corti,[49] G. C. Costantino,[61] J. Cottee Meldrum,[55] B. Couturier,[49] D. C. Craik,[51] N. Crepet,[14] M. Cruz Torres,[2,l] M. Cubero Campos,[9] E. Curras Rivera,[50] R. Currie,[59] C. L. Da Silva,[68] X. Dai,[4] J. Dalseno,[44] C. D'Ambrosio,[62] G. Darze,[3] A. Davidson,[57] J. E. Davies,[63] O. De Aguiar Francisco,[63] C. De Angelis,[32,m] F. De Benedetti,[49] J. de Boer,[38] K. De Bruyn,[83] S. De Capua,[63] M. De Cian,[63] U. De Freitas Carneiro Da Graca,[2] E. De Lucia,[28] J. M. De Miranda,[2] L. De Paula,[3] M. De Serio,[24,n] P. De Simone,[28] F. De Vellis,[19] J. A. de Vries,[84] F. Debernardis,[24] D. Decamp,[10] S. Dekkers,[1] L. Del Buono,[16] B. Delaney,[65] J. Deng,[8] V. Denysenko,[51] O. Deschamps,[11] F. Dettori,[32,m] B. Dey,[80] P. Di Nezza,[28] S. Ding,[69] Y. Ding,[50] L. Dittmann,[22] A. D. Docheva,[60] A. Doheny,[57] C. Dong,[4] F. Dordei,[32] A. C. dos Reis,[2] A. D. Dowling,[69] L. Dreyfus,[13] W. Duan,[73] P. Duda,[86] L. Dufour,[50] V. Duk,[34] P. Durante,[49] M. M. Duras,[86] J. M. Durham,[68] O. D. Durmus,[80] K. Duwe,[49] A. Dziurda,[41] S. Easo,[58] E. Eckstein,[18] U. Egede,[1] S. Eisenhardt,[59] E. Ejopu,[61] L. Eklund,[87] M. Elashri,[66] D. Elizondo Blanco,[9] J. Ellbracht,[19] S. Ely,[62] A. Ene,[43] J. Eschle,[69] T. Evans,[38] F. Fabiano,[14] S. Faghih,[66] L. N. Falcao,[31,c] B. Fang,[7] R. Fantechi,[35] L. Fantini,[34,o] M. Faria,[50] K. Farmer,[59] F. Fassin,[83,38] D. Fazzini,[31,c] L. Felkowski,[86] C. Feng,[6] M. Feng,[5,7] A. Fernandez Casani,[48] M. Fernandez Gomez,[47] A. D. Fernez,[67] F. Ferrari,[25,h] F. Ferreira Rodrigues,[3] M. Ferrillo,[51] M. Ferro-Luzzi,[49] R. A. Fini,[24] M. Fiorini,[26,f] M. Firlej,[40] K. L. Fischer,[64] D. S. Fitzgerald,[89] C. Fitzpatrick,[63] T. Fiutowski,[40] F. Fleuret,[15] A. Fomin,[52] M. Fontana,[25,49] L. A. Foreman,[63] R. Forty,[49] D. Foulds-Holt,[59] V. Franco Lima,[3] M. Franco Sevilla,[67] M. Frank,[49] E. Franzoso,[26,f] G. Frau,[63] C. Frei,[49] D. A. Friday,[63,49] J. Fu,[7] Q. Führing,[19,56,b] T. Fulghesu,[13] G. Galati,[24,n] M. D. Galati,[38] A. Gallas Torreira,[47] D. Galli,[25,h] S. Gambetta,[59] M. Gandelman,[3] P. Gandini,[30] B. Ganie,[63] H. Gao,[7] R. Gao,[64] T. Q. Gao,[56]

Y. Gao,[8] Y. Gao,[6] Y. Gao,[8] L. M. Garcia Martin,[50] P. Garcia Moreno,[45] J. García Pardiñas,[65] P. Gardner,[67] L. Garrido,[45] C. Gaspar,[49] A. Gavrikov,[33] E. Gersabeck,[20] M. Gersabeck,[20] T. Gershon,[57] S. Ghizzo,[29,i] Z. Ghorbanimoghaddam,[55] F. I. Giasemis,[16,p] V. Gibson,[56] H. K. Giemza,[42] A. L. Gilman,[66] M. Giovannetti,[28] A. Gioventù,[47] L. Girardey,[63,58] M. A. Giza,[41] F. C. Glaser,[22] V. V. Gligorov,[16] C. Göbel,[70] L. Golinka-Bezshyyko,[88] E. Golobardes,[46] A. Golutvin,[62,49] S. Gomez Fernandez,[45] W. Gomulka,[40] F. Goncalves Abrantes,[64] I. Gonçales Vaz,[49] M. Goncerz,[41] G. Gong,[4,q] J. A. Gooding,[19] C. Gotti,[31] E. Govorkova,[65] J. P. Grabowski,[30] L. A. Granado Cardoso,[49] E. Graugés,[45] E. Graverini,[35,50] L. Grazette,[57] G. Graziani,[27] A. T. Grecu,[43] N. A. Grieser,[66] L. Grillo,[60] C. Gu,[15] M. Guarise,[26] L. Guerry,[11] A.-K. Guseinov,[50] Y. Guz,[6] T. Gys,[49] K. Habermann,[18] T. Hadavizadeh,[1] C. Hadjivasiliou,[67] G. Haefeli,[50] C. Haen,[49] S. Haken,[56] G. Hallett,[57] P. M. Hamilton,[67] Q. Han,[33] S. Han,[7] X. Han,[22,49] S. Hansmann-Menzemer,[22] N. Harnew,[64] T. J. Harris,[1] M. Hartmann,[14] S. Hashmi,[40] J. He,[7,r] N. Heatley,[14] A. Hedes,[63] F. Hemmer,[49] C. Henderson,[66] R. Henderson,[14] R. D. L. Henderson,[1] A. M. Hennequin,[49] K. Hennessy,[61] J. Herd,[62] P. Herrero Gascon,[22] J. Heuel,[17] A. Heyn,[13] A. Hicheur,[3] G. Hijano Mendizabal,[51] J. Horswill,[63] R. Hou,[8] Y. Hou,[11] D. C. Houston,[60] N. Howarth,[61] W. Hu,[7,r] X. Hu,[4] W. Hulsbergen,[38] R. J. Hunter,[57] D. Hutchcroft,[61] M. Idzik,[40] P. Ilten,[66] A. Iohner,[10] H. Jage,[17] S. J. Jaimes Elles,[77,48,49] S. Jakobsen,[49] T. Jakoubek,[78] E. Jans,[38] A. Jawahery,[67] C. Jayaweera,[54] A. Jelavic,[1] V. Jevtic,[19] Z. Jia,[16] E. Jiang,[67] X. Jiang,[5,7] Y. Jiang,[7] Y. J. Jiang,[6] E. Jimenez Moya,[9] N. Jindal,[91] M. John,[64] A. John Rubesh Rajan,[23] D. Johnson,[54] C. R. Jones,[56] S. Joshi,[42] B. Jost,[49] J. Juan Castella,[56] N. Jurik,[49] I. Juszczak,[41] K. Kalecinska,[40] D. Kaminaris,[50] S. Kandybei,[52] M. Kane,[59] Y. Kang,[4,q] C. Kar,[11] M. Karacson,[49] A. Kauniskangas,[50] J. W. Kautz,[66] M. K. Kazanecki,[41] F. Keizer,[49] M. Kenzie,[56] T. Ketel,[38] B. Khanji,[69] S. Kholodenko,[62,49] G. Khreich,[14] F. Kiraz,[14] T. Kirn,[17] V. S. Kirsebom,[31,c] N. Kleijne,[35,j] A. Kleimenova,[50] D. K. Klekots,[88] K. Klimaszewski,[42] M. R. Kmiec,[42] T. Knospe,[19] R. Kolb,[22] S. Koliiev,[53] L. Kolk,[19] A. Konoplyannikov,[6] P. Kopciewicz,[49] P. Koppenburg,[38] A. Korchin,[52] I. Kostiuk,[38] O. Kot,[53] S. Kotriakhova,[32] E. Kowalczyk,[67] O. Kravcov,[81] M. Kreps,[57] W. Krupa,[49] W. Krzemien,[42] O. Kshyvanskyi,[53] S. Kubis,[86] M. Kucharczyk,[41] A. Kupsc,[87,42] V. Kushnir,[52] B. Kutsenko,[13] J. Kvapil,[68] I. Kyryllin,[52] D. Lacarrere,[49] P. Laguarta Gonzalez,[45] A. Lai,[32] A. Lampis,[32] D. Lancierini,[62] C. Landesa Gomez,[47] J. J. Lane,[1] G. Lanfranchi,[28] C. Langenbruch,[22] T. Latham,[57] F. Lazzari,[35,s] C. Lazzeroni,[54] R. Le Gac,[13] H. Lee,[61] R. Lefèvre,[11] M. Lehuraux,[57] E. Lemos Cid,[49] O. Leroy,[13] T. Lesiak,[41] E. D. Lesser,[68] B. Leverington,[22] A. Li,[4,q] C. Li,[4] C. Li,[13] H. Li,[73] J. Li,[8] K. Li,[76] L. Li,[63] P. Li,[7] P.-R. Li,[74] Q. Li,[5,7] T. Li,[72] T. Li,[73] Y. Li,[8] Y. Li,[5] Y. Li,[4] Z. Lian,[4,q] Q. Liang,[8] X. Liang,[69] Z. Liang,[32] S. Libralon,[48] A. Lightbody,[12] T. Lin,[58] R. Lindner,[49] H. Linton,[62] R. Litvinov,[66] D. Liu,[8] F. L. Liu,[1] G. Liu,[73] K. Liu,[74] S. Liu,[5] W. Liu,[8] Y. Liu,[59] Y. Liu,[74] Y. L. Liu,[62] G. Loachamin Ordonez,[70] I. Lobo,[1] A. Lobo Salvia,[10] A. Loi,[32] T. Long,[56] F. C. L. Lopes,[2,g] J. H. Lopes,[3] A. Lopez Huertas,[45] C. Lopez Iribarnegaray,[47] Q. Lu,[15] C. Lucarelli,[49] D. Lucchesi,[33,t] M. Lucio Martinez,[48] Y. Luo,[6] A. Lupato,[33,u] M. Lupberger,[20] E. Luppi,[26,f] K. Lynch,[23] S. Lyu,[6] X.-R. Lyu,[7] H. Ma,[72] S. Maccolini,[49] F. Machefert,[14] F. Maciuc,[43] B. Mack,[69] I. Mackay,[64] L. M. Mackey,[69] L. R. Madhan Mohan,[56] M. J. Madurai,[54] D. Magdalinski,[38] J. J. Malczewski,[41] S. Malde,[64] L. Malentacca,[49] G. Manca,[32,m] G. Mancinelli,[13] C. Mancuso,[14] R. Manera Escalero,[45] A. Mangalasseri,[80] F. M. Manganella,[37] D. Manuzzi,[25] S. Mao,[7] D. Marangotto,[30,k] J. F. Marchand,[10] R. Marchevski,[50] U. Marconi,[25] E. Mariani,[16] S. Mariani,[49] C. Marin Benito,[45] J. Marks,[22] A. M. Marshall,[55] L. Martel,[64] G. Martelli,[19] G. Martellotti,[36] L. Martinazzoli,[49] M. Martinelli,[31,c] C. Martinez,[3] D. Martinez Gomez,[83] D. Martinez Santos,[44] F. Martinez Vidal,[48] A. Martorell i Granollers,[46] A. Massafferri,[2] R. Matev,[49] A. Mathad,[49] C. Matteuzzi,[69] K. R. Mattioli,[15] A. Mauri,[62] E. Maurice,[15] J. Mauricio,[45] P. Mayencourt,[50] J. Mazorra de Cos,[48] M. Mazurek,[42] D. Mazzanti Tarancon,[45] M. McCann,[62] N. T. McHugh,[60] A. McNab,[63] R. McNulty,[23] B. Meadows,[66] D. Melnychuk,[42] D. Mendoza Granada,[16] P. Menendez Valdes Perez,[47] F. M. Meng,[4,q] M. Merk,[38,84] A. Merli,[50,30] L. Meyer Garcia,[67] D. Miao,[5,7] H. Miao,[30] M. Mikhasenko,[79] D. A. Milanes,[85] A. Minotti,[31,c] E. Minucci,[28] B. Mitreska,[63] D. S. Mitzel,[19] R. Mocanu,[43] A. Modak,[58] L. Moeser,[19] R. D. Moise,[17] E. F. Molina Cardenas,[89] T. Mombächer,[47] M. Monk,[56] T. Monnard,[50] S. Monteil,[11] A. Morcillo Gomez,[47] G. Morello,[28] M. J. Morello,[35,j] M. P. Morgenthaler,[22] A. Moro,[31,c] J. Moron,[40] W. Morren,[38] A. B. Morris,[81,49] A. G. Morris,[13] R. Mountain,[69] Z. Mu,[6] N. Muangkod,[65] E. Muhammad,[57] F. Muheim,[59] M. Mulder,[19]

K. Müller,[51] F. Muñoz-Rojas,[9] V. Mytrochenko,[52] P. Naik,[61] T. Nakada,[50] R. Nandakumar,[58] G. Napoletano,[50] I. Nasteva,[3] M. Needham,[59] N. Neri,[30,k] S. Neubert,[18] N. Neufeld,[49] J. Nicolini,[49] D. Nicotra,[84] E. M. Niel,[15] L. Nisi,[19] Q. Niu,[74] B. K. Njoki,[49] P. Nogarolli,[3] P. Nogga,[18] C. Normand,[47] J. Novoa Fernandez,[47] G. Nowak,[66] H. N. Nur,[60] A. Oblakowska-Mucha,[40] T. Oeser,[17] O. Okhrimenko,[53] R. Oldeman,[32,m] F. Oliva,[59,49] E. Olivart Pino,[45] M. Olocco,[19] R. H. O'Neil,[49] J. S. Ordonez Soto,[11] D. Osthues,[19] J. M. Otalora Goicochea,[3] P. Owen,[51] A. Oyanguren,[48] O. Ozcelik,[49] F. Paciolla,[35,v] A. Padee,[42] K. O. Padeken,[18] B. Pagare,[47] T. Pajero,[49] A. Palano,[24] L. Palini,[30] M. Palutan,[28] C. Pan,[75] X. Pan,[4,q] S. Panebianco,[12] S. Paniskaki,[49] L. Paolucci,[63] A. Papanestis,[58] M. Pappagallo,[24,n] L. L. Pappalardo,[26] C. Pappenheimer,[66] C. Parkes,[63] D. Parmar,[79] G. Passaleva,[27] D. Passaro,[35,j] A. Pastore,[24] M. Patel,[62] J. Patoc,[64] C. Patrignani,[25,h] A. Paul,[69] C. J. Pawley,[84] A. Pellegrino,[38] J. Peng,[5,7] X. Peng,[74] M. Pepe Altarelli,[28] S. Perazzini,[25] H. Pereira Da Costa,[68] M. Pereira Martinez,[47] A. Pereiro Castro,[47] C. Perez,[46] P. Perret,[11] A. Perrevoort,[83] A. Perro,[49] M. J. Peters,[66] K. Petridis,[55] A. Petrolini,[29,i] S. Pezzulo,[29,i] J. P. Pfaller,[66] H. Pham,[69] L. Pica,[35,j] M. Piccini,[34] L. Piccolo,[32] B. Pietrzyk,[10] R. N. Pilato,[61] D. Pinci,[36] F. Pisani,[49] M. Pizzichemi,[31,49,c] V. M. Placinta,[43] M. Plo Casasus,[47] T. Poeschl,[49] F. Polci,[16] M. Poli Lener,[28] A. Poluektov,[13] I. Polyakov,[63] E. Polycarpo,[3] S. Ponce,[49] D. Popov,[7,49] K. Popp,[19] K. Prasanth,[59] C. Prouve,[44] D. Provenzano,[32,49,m] V. Pugatch,[53] A. Puicercus Gomez,[49] G. Punzi,[35,s] J. R. Pybus,[68] Q. Qian,[6] W. Qian,[7] N. Qin,[4,q] R. Quagliani,[49] R. I. Rabadan Trejo,[57] B. Rachwal,[40] R. Racz,[81] J. H. Rademacker,[55] M. Rama,[35] M. Ramírez García,[89] V. Ramos De Oliveira,[70] M. Ramos Pernas,[49] M. S. Rangel,[3] G. Raven,[39] M. Rebollo De Miguel,[48] F. Redi,[30,u] J. Reich,[55] F. Reiss,[20] Z. Ren,[7] P. K. Resmi,[64] M. Ribalda Galvez,[45] R. Ribatti,[50] G. Ricart,[12] D. Riccardi,[35,j] S. Ricciardi,[58] K. Richardson,[65] M. Richardson-Slipper,[56] F. Riehn,[19] K. Rinnert,[61] P. Robbe,[14,49] G. Robertson,[60] E. Rodrigues,[61] A. Rodriguez Alvarez,[45] E. Rodriguez Fernandez,[47] J. A. Rodriguez Lopez,[77] E. Rodriguez Rodriguez,[49] J. Roensch,[19] A. Rogovskiy,[58] D. L. Rolf,[19] P. Roloff,[49] V. Romanovskiy,[66] A. Romero Vidal,[47] G. Romolini,[26,49] F. Ronchetti,[50] T. Rong,[6] M. Rotondo,[28] M. S. Rudolph,[69] M. Ruiz Diaz,[22] J. Ruiz Vidal,[84] J. J. Saavedra-Arias,[9] J. J. Saborido Silva,[47] S. E. R. Sacha Emile R.,[49] D. Sahoo,[80] N. Sahoo,[54] B. Saitta,[32] M. Salomoni,[31,49,c] I. Sanderswood,[48] R. Santacesaria,[36] C. Santamarina Rios,[47] M. Santimaria,[28] L. Santoro,[2] E. Santovetti,[37] A. Saputi,[26,49] A. Sarnatskiy,[83] G. Sarpis,[49] M. Sarpis,[81] C. Satriano,[36] A. Satta,[37] M. Saur,[74] H. Sazak,[17] F. Sborzacchi,[49,28] A. Scarabotto,[19] S. Schael,[17] S. Scherl,[61] M. Schiller,[22] H. Schindler,[49] M. Schmelling,[21] B. Schmidt,[49] N. Schmidt,[68] S. Schmitt,[65] H. Schmitz,[18] O. Schneider,[50] A. Schopper,[62] N. Schulte,[19] M. H. Schune,[14] G. Schwering,[17] B. Sciascia,[28] A. Sciuccati,[49] G. Scriven,[84] I. Segal,[79] S. Sellam,[47] M. Senghi Soares,[39] A. Sergi,[29,i] N. Serra,[51] L. Sestini,[27] B. Sevilla Sanjuan,[46] Y. Shang,[6] D. M. Shangase,[89] R. S. Sharma,[69] L. Shchutska,[50] T. Shears,[61] J. Shen,[6] Z. Shen,[38] S. Sheng,[50] B. Shi,[7] J. Shi,[56] Q. Shi,[7] W. S. Shi,[73] E. Shmanin,[25] R. Silva Coutinho,[2] G. Simi,[33,t] S. Simone,[24,n] M. Singha,[80] I. Siral,[50] N. Skidmore,[57] T. Skwarnicki,[69] M. W. Slater,[54] E. Smith,[65] M. Smith,[62] L. Soares Lavra,[59] M. D. Sokoloff,[66] F. J. P. Soler,[60] A. Solomin,[55] K. Solovieva,[20] N. S. Sommerfeld,[18] R. Song,[1] Y. Song,[50] Y. Song,[4,q] Y. S. Song,[6] F. L. Souza De Almeida,[45] B. Souza De Paula,[3] K. M. Sowa,[40] E. Spadaro Norella,[29,i] E. Spedicato,[25] J. G. Speer,[19] P. Spradlin,[60] F. Stagni,[49] M. Stahl,[79] S. Stahl,[49] S. Stanislaus,[64] M. Stefaniak,[91] O. Steinkamp,[51] F. Suljik,[64] J. Sun,[63] L. Sun,[75] M. Sun,[6] D. Sundfeld,[2] W. Sutcliffe,[51] P. Svihra,[78] V. Svintozelskyi,[48] K. Swientek,[40] F. Swystun,[56] A. Szabelski,[42] T. Szumlak,[40] Y. Tan,[7] Y. Tang,[75] Y. T. Tang,[7] M. D. Tat,[22] J. A. Teijeiro Jimenez,[47] F. Terzuoli,[35,v] F. Teubert,[49] E. Thomas,[49] D. J. D. Thompson,[54] A. R. Thomson-Strong,[59] H. Tilquin,[62] V. Tisserand,[11] S. T'Jampens,[10] M. Tobin,[5,49] T. T. Todorov,[20] L. Tomassetti,[26,f] G. Tonani,[30] X. Tong,[6] T. Tork,[30] L. Toscano,[19] D. Y. Tou,[4,q] C. Trippl,[46] G. Tuci,[22] N. Tuning,[38] L. H. Uecker,[22] A. Ukleja,[40] A. Upadhyay,[49] B. Urbach,[59] A. Usachov,[38] U. Uwer,[22] V. Vagnoni,[25,49] A. Vaitkevicius,[81] V. Valcarce Cadenas,[47] G. Valenti,[25] N. Valls Canudas,[49] J. van Eldik,[49] H. Van Hecke,[68] E. van Herwijnen,[62] C. B. Van Hulse,[47,w] R. Van Laak,[50] M. van Veghel,[84] G. Vasquez,[51] R. Vazquez Gomez,[45] P. Vazquez Regueiro,[47] C. Vázquez Sierra,[44] S. Vecchi,[26] J. Velilla Serna,[48] J. J. Velthuis,[55] M. Veltri,[27,x] A. Venkateswaran,[50] M. Verdoglia,[32] M. Vesterinen,[57] W. Vetens,[69] D. Vico Benet,[64] P. Vidrier Villalba,[45] M. Vieites Diaz,[47] X. Vilasis-Cardona,[46] E. Vilella Figueras,[61] A. Villa,[50] P. Vincent,[16] B. Vivacqua,[3] F. C. Volle,[54] D. vom Bruch,[13] K. Vos,[84] C. Vrahas,[59] J. Wagner,[19] J. Walsh,[35] N. Walter,[49]

E. J. Walton,[1] G. Wan,[6] A. Wang,[7] B. Wang,[5] C. Wang,[22] G. Wang,[8] H. Wang,[74] J. Wang,[7] J. Wang,[5] J. Wang,[4,q] J. Wang,[75] M. Wang,[49] N. W. Wang,[7] R. Wang,[55] X. Wang,[8] X. Wang,[73] X. Wang,[4] X. W. Wang,[62] Y. Wang,[76] Y. Wang,[6] Y. H. Wang,[74] Z. Wang,[14] Z. Wang,[30] J. A. Ward,[57,1] M. Waterlaat,[49] N. K. Watson,[54] D. Websdale,[62] Y. Wei,[6] Z. Weida,[7] J. Wendel,[44] B. D. C. Westhenry,[55] C. White,[56] M. Whitehead,[60] E. Whiter,[54] A. R. Wiederhold,[63] D. Wiedner,[19] M. A. Wiegertjes,[38] C. Wild,[64] G. Wilkinson,[64] M. K. Wilkinson,[66] M. Williams,[65] M. J. Williams,[49] M. R. J. Williams,[59] R. Williams,[56] S. Williams,[55] Z. Williams,[55] F. F. Wilson,[58] M. Winn,[12] W. Wislicki,[42] M. Witek,[41] L. Witola,[19] T. Wolf,[22] E. Wood,[56] G. Wormser,[14] S. A. Wotton,[56] H. Wu,[69] J. Wu,[8] X. Wu,[75] Y. Wu,[6,56] Z. Wu,[7] K. Wyllie,[49] S. Xian,[73] Z. Xiang,[5] Y. Xie,[8] T. X. Xing,[30] A. Xu,[35,j] L. Xu,[4,q] M. Xu,[49] R. Xu,[89] Z. Xu,[49] Z. Xu,[92] Z. Xu,[7] Z. Xu,[5] S. Yadav,[26] K. Yang,[62] X. Yang,[6] Y. Yang,[7] Y. Yang,[80] Z. Yang,[6] Z. Yang,[4] H. Yeung,[63] H. Yin,[8] X. Yin,[7] C. Y. Yu,[6] J. Yu,[72] X. Yuan,[5] Y Yuan,[5,7] J. A. Zamora Saa,[71] M. Zavertyaev,[21] M. Zdybal,[41] F. Zenesini,[25] C. Zeng,[5,7] M. Zeng,[4,q] S. H Zeng,[55] C. Zhang,[6] D. Zhang,[7] D. Zhang,[8] J. Zhang,[42] L. Zhang,[4,q] L. Zhang,[49] R. Zhang,[8] S. Zhang,[64] S. L. Zhang,[72] Y. Zhang,[6] Z. Zhang,[4,q] J. Zhao,[7] Y. Zhao,[22] A. Zhelezov,[22] S. Z. Zheng,[6] X. Z. Zheng,[4,q] Y. Zheng,[7] T. Zhou,[41] X. Zhou,[8] V. Zhovkovska,[57] L. Z. Zhu,[59] X. Zhu,[4,q] X. Zhu,[8] Y. Zhu,[17] V. Zhukov,[17] J. Zhuo,[48] D. Zuliani,[33,t] and G. Zunica[28]

(LHCb Collaboration)

[1]*School of Physics and Astronomy, Monash University, Melbourne, Australia*
[2]*Centro Brasileiro de Pesquisas Físicas (CBPF), Rio de Janeiro, Brazil*
[3]*Universidade Federal do Rio de Janeiro (UFRJ), Rio de Janeiro, Brazil*
[4]*Department of Engineering Physics, Tsinghua University, Beijing, China*
[5]*Institute of High Energy Physics (IHEP), Beijing, China*
[6]*School of Physics State Key Laboratory of Nuclear Physics and Technology, Peking University, Beijing, China*
[7]*University of Chinese Academy of Sciences, Beijing, China*
[8]*Institute of Particle Physics, Central China Normal University, Wuhan, Hubei, China*
[9]*Consejo Nacional de Rectores (CONARE), San Jose, Costa Rica*
[10]*Université Savoie Mont Blanc, CNRS, IN2P3-LAPP, Annecy, France*
[11]*Université Clermont Auvergne, CNRS/IN2P3, LPC, Clermont-Ferrand, France*
[12]*Université Paris-Saclay, Centre d'Etudes de Saclay (CEA), IRFU, Gif-Sur-Yvette, France*
[13]*Aix Marseille University, CNRS/IN2P3, CPPM, Marseille, France*
[14]*Université Paris-Saclay, CNRS/IN2P3, IJCLab, Orsay, France*
[15]*Laboratoire Leprince-Ringuet, CNRS/IN2P3, Ecole Polytechnique, Institut Polytechnique de Paris, Palaiseau, France*
[16]*Laboratoire de Physique Nucléaire et de Hautes Énergies (LPNHE), Sorbonne Université, CNRS/IN2P3, Paris, France*
[17]*I. Physikalisches Institut, RWTH Aachen University, Aachen, Germany*
[18]*Universität Bonn—Helmholtz-Institut für Strahlen und Kernphysik, Bonn, Germany*
[19]*Fakultät Physik, Technische Universität Dortmund, Dortmund, Germany*
[20]*Physikalisches Institut, Albert-Ludwigs-Universität Freiburg, Freiburg, Germany*
[21]*Max-Planck-Institut für Kernphysik (MPIK), Heidelberg, Germany*
[22]*Physikalisches Institut, Ruprecht-Karls-Universität Heidelberg, Heidelberg, Germany*
[23]*School of Physics, University College Dublin, Dublin, Ireland*
[24]*INFN Sezione di Bari, Bari, Italy*
[25]*INFN Sezione di Bologna, Bologna, Italy*
[26]*INFN Sezione di Ferrara, Ferrara, Italy*
[27]*INFN Sezione di Firenze, Firenze, Italy*
[28]*INFN Laboratori Nazionali di Frascati, Frascati, Italy*
[29]*INFN Sezione di Genova, Genova, Italy*
[30]*INFN Sezione di Milano, Milano, Italy*
[31]*INFN Sezione di Milano-Bicocca, Milano, Italy*
[32]*INFN Sezione di Cagliari, Monserrato, Italy*
[33]*INFN Sezione di Padova, Padova, Italy*
[34]*INFN Sezione di Perugia, Perugia, Italy*
[35]*INFN Sezione di Pisa, Pisa, Italy*
[36]*INFN Sezione di Roma La Sapienza, Roma, Italy*
[37]*INFN Sezione di Roma Tor Vergata, Roma, Italy*

[38]Nikhef National Institute for Subatomic Physics, Amsterdam, Netherlands
[39]Nikhef National Institute for Subatomic Physics and VU University Amsterdam, Amsterdam, Netherlands
[40]AGH - University of Krakow, Faculty of Physics and Applied Computer Science, Kraków, Poland
[41]Henryk Niewodniczanski Institute of Nuclear Physics Polish Academy of Sciences, Kraków, Poland
[42]National Center for Nuclear Research (NCBJ), Warsaw, Poland
[43]Horia Hulubei National Institute of Physics and Nuclear Engineering, Bucharest-Magurele, Romania
[44]Universidade da Coruña, A Coruña, Spain
[45]ICCUB, Universitat de Barcelona, Barcelona, Spain
[46]La Salle, Universitat Ramon Llull, Barcelona, Spain
[47]Instituto Galego de Física de Altas Enerxías (IGFAE), Universidade de Santiago de Compostela, Santiago de Compostela, Spain
[48]Instituto de Fisica Corpuscular, Centro Mixto Universidad de Valencia—CSIC, Valencia, Spain
[49]European Organization for Nuclear Research (CERN), Geneva, Switzerland
[50]Institute of Physics, Ecole Polytechnique Fédérale de Lausanne (EPFL), Lausanne, Switzerland
[51]Physik-Institut, Universität Zürich, Zürich, Switzerland
[52]NSC Kharkiv Institute of Physics and Technology (NSC KIPT), Kharkiv, Ukraine
[53]Institute for Nuclear Research of the National Academy of Sciences (KINR), Kyiv, Ukraine
[54]School of Physics and Astronomy, University of Birmingham, Birmingham, United Kingdom
[55]H.H. Wills Physics Laboratory, University of Bristol, Bristol, United Kingdom
[56]Cavendish Laboratory, University of Cambridge, Cambridge, United Kingdom
[57]Department of Physics, University of Warwick, Coventry, United Kingdom
[58]STFC Rutherford Appleton Laboratory, Didcot, United Kingdom
[59]School of Physics and Astronomy, University of Edinburgh, Edinburgh, United Kingdom
[60]School of Physics and Astronomy, University of Glasgow, Glasgow, United Kingdom
[61]Oliver Lodge Laboratory, University of Liverpool, Liverpool, United Kingdom
[62]Imperial College London, London, United Kingdom
[63]Department of Physics and Astronomy, University of Manchester, Manchester, United Kingdom
[64]Department of Physics, University of Oxford, Oxford, United Kingdom
[65]Massachusetts Institute of Technology, Cambridge, Massachusetts, USA
[66]University of Cincinnati, Cincinnati, Ohio, USA
[67]University of Maryland, College Park, Maryland, USA
[68]Los Alamos National Laboratory (LANL), Los Alamos, New Mexico, USA
[69]Syracuse University, Syracuse, New York, USA
[70]Pontifícia Universidade Católica do Rio de Janeiro (PUC-Rio), Rio de Janeiro, Brazil (associated with Universidade Federal do Rio de Janeiro (UFRJ), Rio de Janeiro, Brazil)
[71]Universidad Andres Bello, Santiago, Chile (associated with Physik-Institut, Universität Zürich, Zürich, Switzerland)
[72]School of Physics and Electronics, Hunan University, Changsha City, China (associated with Institute of Particle Physics, Central China Normal University, Wuhan, Hubei, China)
[73]State Key Laboratory of Nuclear Physics and Technology, South China Normal University, Guangzhou, China (associated with Department of Engineering Physics, Tsinghua University, Beijing, China)
[74]Lanzhou University, Lanzhou, China (associated with Institute of High Energy Physics (IHEP), Beijing, China)
[75]School of Physics and Technology, Wuhan University, Wuhan, China (associated with Department of Engineering Physics, Tsinghua University, Beijing, China)
[76]Henan Normal University, Xinxiang, China (associated with Institute of Particle Physics, Central China Normal University, Wuhan, Hubei, China)
[77]Departamento de Fisica, Universidad Nacional de Colombia, Bogota, Colombia (associated with Laboratoire de Physique Nucléaire et de Hautes Énergies (LPNHE), Sorbonne Université, CNRS/IN2P3, Paris, France)
[78]Institute of Physics of the Czech Academy of Sciences, Prague, Czech Republic (associated with Department of Physics and Astronomy, University of Manchester, Manchester, United Kingdom)
[79]Ruhr Universitaet Bochum, Fakultaet für Physik und Astronomie, Bochum, Germany (associated with Fakultät Physik, Technische Universität Dortmund, Dortmund, Germany)
[80]Eotvos Lorand University, Budapest, Hungary (associated with European Organization for Nuclear Research (CERN), Geneva, Switzerland)
[81]Faculty of Physics, Vilnius University, Vilnius, Lithuania (associated with Physikalisches Institut, Albert-Ludwigs-Universität Freiburg, Freiburg, Germany)
[82]Institute of Physics and Technology, Ulan Bator, Mongolia (associated with Institute of High Energy Physics (IHEP), Beijing, China)
[83]Van Swinderen Institute, University of Groningen, Groningen, Netherlands (associated with Nikhef National Institute for Subatomic Physics, Amsterdam, Netherlands)

[84]*Universiteit Maastricht, Maastricht, Netherlands*
(associated with Nikhef National Institute for Subatomic Physics, Amsterdam, Netherlands)
[85]*Universidad de Ingeniería y Tecnología (UTEC), Lima, Peru*
(associated with Massachusetts Institute of Technology, Cambridge, Massachusetts, USA)
[86]*Tadeusz Kosciuszko Cracow University of Technology, Cracow, Poland*
(associated with Henryk Niewodniczanski Institute of Nuclear Physics Polish Academy of Sciences, Kraków, Poland)
[87]*Department of Physics and Astronomy, Uppsala University, Uppsala, Sweden*
(associated with School of Physics and Astronomy, University of Glasgow, Glasgow, United Kingdom)
[88]*Taras Schevchenko University of Kyiv, Faculty of Physics, Kyiv, Ukraine*
(associated with Université Paris-Saclay, CNRS/IN2P3, IJCLab, Orsay, France)
[89]*University of Michigan, Ann Arbor, Michigan, USA (associated with Syracuse University, Syracuse, New York, USA)*
[90]*Indiana University, Bloomington, Indiana, USA*
(associated with Los Alamos National Laboratory (LANL), Los Alamos, New Mexico, USA)
[91]*Ohio State University, Columbus, Ohio, USA*
(associated with Los Alamos National Laboratory (LANL), Los Alamos, New Mexico, USA)
[92]*Kent State University, Physics Department, Kent, Ohio, USA*
(associated with Los Alamos National Laboratory (LANL), Los Alamos, New Mexico, USA)

[a]Deceased.
[b]Also at Lamarr Institute for Machine Learning and Artificial Intelligence, Dortmund, Germany.
[c]Also at Università degli Studi di Milano-Bicocca, Milano, Italy.
[d]Also at Università di Modena e Reggio Emilia, Modena, Italy.
[e]Also at Department of Physics and Astronomy, University of Victoria, Victoria, Canada.
[f]Also at Università di Ferrara, Ferrara, Italy.
[g]Also at Universidade Estadual de Campinas (UNICAMP), Campinas, Brazil.
[h]Also at Università di Bologna, Bologna, Italy.
[i]Also at Università di Genova, Genova, Italy.
[j]Also at Scuola Normale Superiore, Pisa, Italy.
[k]Also at Università degli Studi di Milano, Milano, Italy.
[l]Also at Universidad Nacional Autónoma de Honduras, Tegucigalpa, Honduras.
[m]Also at Università di Cagliari, Cagliari, Italy.
[n]Also at Università di Bari, Bari, Italy.
[o]Also at Università di Perugia, Perugia, Italy.
[p]Also at LIP6, Sorbonne Université, Paris, France.
[q]Also at Center for High Energy Physics, Tsinghua University, Beijing, China.
[r]Also at Hangzhou Institute for Advanced Study, UCAS, Hangzhou, China.
[s]Also at Università di Pisa, Pisa, Italy.
[t]Also at Università di Padova, Padova, Italy.
[u]Also at Università di Bergamo, Bergamo, Italy.
[v]Also at Università di Siena, Siena, Italy.
[w]Also at Universidad de Alcalá, Alcalá de Henares, Spain.
[x]Also at Università di Urbino, Urbino, Italy.